# Stim-activated TRPC-ORAI channels in pulmonary hypertension induced by chronic intermittent hypoxia

Sebastian Castillo-Galán[1], German A. Arenas[1], Roberto V. Reyes[2], Bernardo J. Krause[3] and Rodrigo Iturriaga[1]

[1]Laboratorio de Neurobiología, Facultad de Ciencias Biológicas, Pontificia Universidad Católica de Chile, Santiago, Chile; [2]Laboratorio de Bioquímica y Biología Molecular de la Hipoxia, Universidad de Chile, Santiago, Chile; [3]Instituto de Ciencias de la Salud, Universidad de O'Higgins, Rancagua, Chile

## Abstract

Obstructive sleep apnea (OSA), a breathing disorder featured by chronic intermittent hypoxia (CIH) is associated with pulmonary hypertension (PH). Rodents exposed to CIH develop pulmonary vascular remodeling and PH, but the pathogenic mechanisms are not well known. Overexpression of Stim-activated Transient Receptor Potential Channels (TRPC) and Calcium Release-Activated Calcium Channel Protein (ORAI) TRPC-ORAI $Ca^{2+}$ channels (STOC) has been involved in pulmonary vascular remodeling and PH in sustained hypoxia. However, it is not known if CIH may change STOC levels. Accordingly, we studied the effects of CIH on the expression of STOC subunits in the lung and if these changes paralleled the progression of the vascular pulmonary remodeling and PH in a preclinical model of OSA. Male Sprague-Dawley rats ($\sim$200 g) were exposed to CIH (5%$O_2$, 12 times/h for 8 h) for 14, 21, and 28 days. We measured right ventricular systolic pressure (RVSP), cardiac morphometry with MRI, pulmonary vascular remodeling, and wire-myographic arterial responses to KCl and endothelin-1 (ET-1). Pulmonary RNA and protein STOC levels of TRPC1, TRPC4, TRPC6, ORAI 1, ORAI 2, and STIM1 subunits were measured by qPCR and western blot, and results were compared with age-matched controls. CIH elicited a progressive increase of RVSP and vascular contractile responses to KCl and ET-1, leading to vascular remodeling and augmented right ventricular ejection fraction, which was significant at 28 days of CIH. The levels of TRPC1, TRPC4, TRPC 6, ORAI 1, and STIM 1 channels increased following CIH, and some of them paralleled morphologic and functional changes. Our findings show that CIH increased pulmonary STOC expression, paralleling vascular remodeling and PH.

## Introduction

Obstructive sleep apnea (OSA) is a major public health problem. Indeed, 10% of adult men and 5% of women worldwide population display an apnea/hypopnea index of 10 or more events/h.[1,2] OSA is associated with somnolence, sleep fragmentation, and cognitive dysfunction.[3] However, OSA is also considered an independent risk factor for systemic diurnal hypertension, and is associated with pulmonary hypertension (PH), stroke, and atrial fibrillation.[2,4,5] Indeed, OSA is associated with moderate PH in the absence of lung pathologies, with an incidence ranging from 20% to 50%.[6–9]

In OSA patients, during sleep, the upper airways collapse eliciting complete or partial airflow detention. The resulting hypoxia and hypercapnia stimulate the carotid body chemoreceptors, evoking cardiorespiratory and sympathetic responses, and finally a microarousal. Among these alterations, chronic intermittent hypoxia (CIH) is thought to be the main factor for developing systemic hypertension.[2,4] Moreover, CIH is sufficient to produce sympathetic overflow and systemic hypertension in animal models of OSA.[10,11] In addition, CIH exposure for long periods (28

Corresponding author:
R. Iturriaga, Laboratorio de Neurobiología, Facultad de Ciencias Biológicas, Pontificia Universidad Católica de Chile, Santiago, Chile.
Email: riturriaga@bio.puc.cl

days) produced vascular lung remodeling and increased the right ventricular systolic pressure (RVSP > 30 mmHg) in rats.[12–14] On the other hand, although the link between OSA and PH is well recognized, the underlying pathogenic mechanisms are not entirely known. It has been suggested that lung hypoxia, oxidative stress, pro-inflammatory molecules, inducible hypoxic factors, and sympathetic- renin-angiotensin system may contribute to the CIH-mediated pulmonary alterations.[12–15]

The chronic exposure to sustained hypoxia elicits vascular remodeling characterized by hypertrophy and/or hyperplasia of pulmonary arterial smooth muscle cells (PASMC), leading to vasoconstriction, augmented pulmonary vascular resistance, and PH.[16,17] The increased intracellular calcium concentration $[Ca^{2+}i]$ plays a key role in the contraction, differentiation, and proliferation of vascular smooth muscle cells induced by sustained hypoxia.[17,18] Among the channels and transporters involved in calcium homeostasis, the Stim-activated TRPC-ORAI $Ca^{2+}$ channels (STOC) play a crucial role in pulmonary arterial vasoconstriction, PASMC proliferation, and the development of PH in animals exposed to sustained hypoxia.[18–20] The STOC are mainly composed of homo or heterotetramer of pore-forming subunits belonging to the TRPC family 1, 4, 6, and /or the family ORAI 1 and 2.[18] On the other hand, an auxiliary subunit, the stromal interaction molecule family 1 (STIM 1), participates as a calcium sensor activating the pore-forming subunits in response to $Ca^{2+}$ depletion of sarcoplasmic reticulum.[21,22] In recent years, attention has been focused on the role played by STOC in the physiology and pathophysiology of pulmonary circulation. Indeed, a growing body of evidence suggest that Stim-activated TRPC-ORAI channels are overexpressed in the lung, pulmonary arteries, and PASMC under sustained hypoxia and play a key role in the development of pulmonary vascular remodeling and over-constriction in pulmonary hypertension development.[23–30] However, to the best of our knowledge, the time course of development of cardiopulmonary disturbances associated to pulmonary hypertension, as well as the effects of different times of CIH exposure on the pulmonary expression of STOC subunits have not been studied. Accordingly, we assessed in a model of OSA, the progressive effects of CIH on vascular pulmonary remodeling, arterial contractile responses ex vivo, RVSP and changes of lung STOC expression, and lung tissue RNA and protein levels of the STOC forming subunits TRPC1, TRPC4, TRPC6, ORAI 1, ORAI 2, and STIM1.

## Methods

### Animals and intermittent hypoxia protocol

Experiments were performed on 32 male Sprague-Dawley rats weighting ~200 g fed with standard diet ad libitum and kept on a 12:12-hour light/dark cycle. Room temperature was maintained between 23°C and 25°C. All the experimental procedures were approved by the Scientific Ethical Committee for the animal and environment care from the Pontificia Universidad Católica de Chile, Santiago, Chile, and were performed according to the National Institutes of Health Guide (NIH, USA) for the care and use of animals. Rats were obtained from the Animal Facility of the Center from Innovation in Biomedical Experimental Models Pontificia Universidad Católica de Chile. Unrestrained, freely moving rats were housed in individual chambers and exposed to hypoxic cycles of 5% inspired $O_2$ for 20 s, followed by 280 s of room air, 12 times per hour for 8 h a day for 14, 21, and 28 days.[31–33] Rats were exposed to CIH from 8:00 a.m. to 4:00 p.m. The $O_2$ level inside the chambers was continuously monitored with an oxygen analyzer (Ohmeda 5120, BOC Healthcare, Manchester, UK).

### In vivo magnetic resonance imaging

Cardiovascular magnetic resonance imaging (MRI) was performed on a preclinical 1.0T Bruker ICON MR scan (Bruker BioSpin, Fällanden, Switzerland) with a gradient strength of 450 mT/m and a solenoid micro-coil. Animal anesthesia was induced with 5% isoflurane and maintained with 1% to 2% isoflurane in $O_2$ during the MRI measurements. Body temperature was controlled using a warm water pump (SA Instruments, Stony Brook, NY, USA). Electrocardiogram was achieved via two metallic needles placed subcutaneously in the front paws, and a pressure transducer was placed on the abdomen for respiratory recording (SA Instruments). Cine-FLASH was used to acquire temporally resolved T1-weighted long and short-axis images of the heart to derive functional and volumetric parameters. Imaging parameters included repetition time (TR), echo time (TE), field of view (FOV), and slice thickness, while TR = RR-interval/number of frames (typically: 8 to 10 ms), TReff = RR-interval, TE = 1.0 ms, FOV = 25 × 25 mm, matrix size = 128 × 128, slice thickness = 1 mm; flip angle = 40°, four averages, nine slices, 1 k-space line/frame, the number of frames per cardiac cycle varied between 10 and 14 to maintain an adequate TR. The acquisition time was 8 ± 0.5 min. The trigger was positioned at the peak of the QRS complex. The phase encoding steps were equally distributed along the cardiac cycle to obtain diastolic and systolic frames for the measurement of functional and volumetric parameters. Ejection fraction (EF) which was an end-systole dimension divided by end-diastole dimension, and end-diastolic and systolic volumes for the right and left ventricles which were measured in a mid-ventricular slice, were estimated. Diameters were given as endocardial diameters and evaluated in a septolateral direction, crossing the interventricular septum orthogonally. Analyses were performed using the same images in OsiriX MD v.9.5 (DICOM viewer and image-analysis program, Pixmeo SARL; Bernex, Switzerland) by two persons independently.[34]

## Right ventricular systolic pressure and heart rate measurements

Rats were anesthetized with urethane (Sigma-Aldrich, St Louis MI, USA; 800 mg/kg i.p.), placed in supine, tracheotomized and connected to a positive pressure ventilator ventilation (RoVent Jr, Kent Scientific, Torrington, CT, USA). The chest was open and a catheter filled with heparinized saline (500 IU/mL) was placed into the right ventricle and connected to a Statham P23 transduced (Hato Rey, Puerto Rico) to measure right ventricle systolic pressure (RVSP). Heart rate (HR) was obtained from the pressure signal recorded a Power Lab 16/35 (ADInstruments, New South Wales, Australia).

## Wire myography

One lung was removed and immediately immersed in cold $1 \times$ phosphate-buffered saline (PBS) solution. Small arteries (2nd generation 300–400 μm) were dissected from the right lobules and mounted on a wire myograph (model 610 A; Danish Myo Technology A/S, Denmark).[32,33] The arteries were maintained at 37°C and equilibrated with 95% $O_2$–5% $CO_2$ in Krebs buffer at pH 7.4. The internal diameter of vessels was defined by determining the stretch condition at which the maximal contractile response to KCl was obtained.[35,36] This ex vivo method has been shown to accurately represent the in vivo internal arterial perimeter in different models.[35,36] Likewise, through this methodology, a direct correlation of the ex vivo contractile response with the biomechanical and structural properties of different blood vessels has been observed.[37] Concentration–response curves (CRCs) were constructed with KCl (Winkler, Santiago, Chile; 6.25 to 125 mM) and endothelin-1 (ET-1, Sigma-Aldrich; $10^{-12}$ to $10^{-6}$ M). The responses were recorded 5 min after each addition. Contractile responses were expressed in terms of tension (N/m) or percentage relative to the tension evoked by a submaximal dose of KCl (40 mM) to normalize for differences arising from variability between different vessels analyzed. CRCs were analyzed in terms of sensitivity and maximal responses by fitting experimental data to the Boltzmann equation or an agonist-response function as appropriate (Prism 5.0; GraphPad Software, La Jolla, CA, USA).

## Histological staining

Immediately after the removal of the lung, two slices of ~1 cm$^3$ axial tissue were removed from the left lung and fixed by immersion with 4% paraformaldehyde for 24 h at 4°C, and followed by conservation in sodium azide 0.01% in PBS $1 \times$ at 4°C. Then the rest of the left lungs were stored at −80°C for molecular analyses. Afterward, the fixed tissue was embedded in paraffin, cut into 4 to 5 μm serial axial slices, and staining with van Gieson for vascular morphometry. The percentage of wall thickness for the small pulmonary arteries (150–250 μm of internal diameter) was calculated as previously described.[38] Briefly, the percentage of vascular smooth muscle was calculated as follows: muscle area (%) = [(external muscle area − internal area)/external muscle area] × 100, where the external muscle area and the internal area are the external and internal boundaries of the tunica media, respectively. Images were captured at 40–100× with a microscope Olympus BX-41 coupled (Olympus, Shinjuku-ku, Tokyo, Japan) to a digital camera and a computer. Ten to fifteen representative small pulmonary arteries from each animal were selected for these analyses. The analysis of the microphotographs was performed with the software Image Pro-Plus 6.2 (Media Cybernetics, Inc., Rockville, MD, USA).

## mRNA extraction and qRT-PCR

Frozen lung samples (~100 mg) were homogenized in TRIzol (Thermo Fisher, Waltham, MA, USA). RNA was resuspended in nuclease-free water and the absorbance was measured at 260 and 280 nm. The 260/280 absorbance ratio was 1.9–2.05. The RNA was stored at −80°C until use. The cDNA synthesis was transcribed through OneScript cDNA Synthesis Kit (ABM, Richmond, Canada). Gene expression of TRPC1, TRPC4, TRPC6, ORAI1, ORAI2, and 18S was quantified through quantitative realtime PCR (qRTPCR) in StepOne Plus (Applied Biosystems, Foster City, CA, USA), using KicqStart Kit (Sigma-Aldrich; see Table 1). All procedures were realized according to the manufacturer's protocol. The relative expressions were calculated using the $2-\Delta\Delta Ct$ method. The control group was used as reference and 18S gene as housekeeper.

## Western blotting

Total proteins from frozen left lung samples were isolated using a RIPA lysis buffer (Thermo Fisher) supplemented with a Protease inhibitor tablet cocktail according to manufacturer's instructions (Pierce™, Thermo Fisher). Protein concentrations were calculated using DC Protein Assay (Bio-Rad Hercules, CA, USA) following the manufacture instructions. Isolated proteins were stored at −80°C until use. Ten micrograms of protein were resolved in an SDS-PAGE (10–12% gradient gels) followed by transferring of proteins onto nitrocellulose membranes. After appropriate blocking (5% nonfat dried milk) the blots were probed with primary antibodies for TRPC1 (Santa Cruz, Dallas, TX, USA, sc-133076), TRPC6 (Santa Cruz, sc-515837), STIM1 (Santa Cruz, sc-166840), ORAI2 (Santa Cruz, sc-376757), and ORAI1 (Santa Cruz, sc-377281), diluted 1:1000 in 5% powdered nonfat dry milk overnight at 4°C. After washing, membranes were incubated with horseradish peroxidase-conjugated secondary anti-mouse antibody (Jackson ImmunoResearch, West Grove, PA, USA) diluted 1:5000 in 5% powdered nonfat dry milk. Levels of proteins were normalized to the β-actin (Sigma-Aldrich, AC-74) content

**Table 1.** Primers sequence's characteristics uses in the analysis.

| Gene | F/R | Primer sequence (5′–3′) | Tm (°C) | Product length (bp) | Extension Time (s) |
|------|-----|-------------------------|---------|---------------------|--------------------|
| TRPC1 | For | 5′-AGTTCCTGAACACCGTTTGG-3′ | 60° | 164 bp | 10 s |
| | Rev | 5′-CGGTGTGTGAATGATTCTGC-3′ | | | |
| TRPC4 | For | 5′-CAGGCTGGAGGAGAAGACAC-3′ | 60° | 195 bp | 10 s |
| | Rev | 5′-AGGCTAGCAGCAGCAGAAAC-3′ | | | |
| TRPC6 | For | 5′-TCTGGCTGCTCATTGCCAGGAATA-3′ | 60° | 323 bp | 30 s |
| | Rev | 5′-AGAGTGGCTGAAGGAGTCATGCTT-3′ | | | |
| ORAI1 | For | 5′-CGCCCTCATGATCAGTACCT-3′ | 60° | 191 bp | 10 s |
| | Rev | 5′-AGAACTTCACCCAGCAGAGC-3′ | | | |
| ORAI2 | For | 5′-GTGGGTCTCATCTTCGTGGT-3′ | 62° | 142 bp | 10 s |
| | Rev | 5′-CCACCTGTAGGCTTCTCTCG-3′ | | | |
| 18S | For | 5′-GTAACCCGTTGAACCCCATT-3′ | 58° | 152 bp | 10 s |
| | Rev | 5′-CCATCCAATCGGTAGTAGCG-3′ | | | |
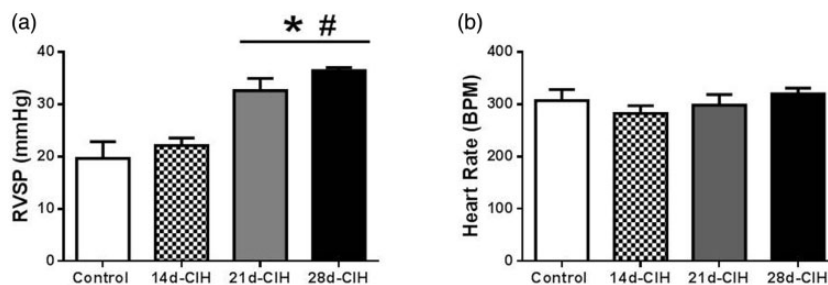


**Fig. 1.** Effect of CIH on right ventricular systolic pressure and heart rate in rats. (a) Right ventricular systolic pressure (RVSP) and (b) heart rate (HR) in control (empty bar $n = 4$) and rats exposed to 14d-CIH (lined bar, $n = 5$), 21d-CIH (gray bar, $n = 4$) and 28d-CIH (black bar, $n = 4$). Values are mean $\pm$ SE. *$p < 0.05$ vs. control, #$p < 0.05$ vs. 14d-CIH. One-way ANOVA and Newman–Keuls post-test.

of the same sample. The signals obtained were scanned with densitometry through a detection device by chemiluminescence (Odyssey Imaging System LI-COR Biosciences, Lincoln, NE, USA) quantified with the Image J software (NIH, Bethesda, MD, USA).

## Statistical analysis

Data are expressed as means $\pm$ SE. Groups were compared by two-way ANOVA and the post hoc Newman–Keuls test or by Student's $t$ test for unpaired data, as appropriate. For all comparisons, differences were considered statistically significant when $p < 0.05$.[39]

## Results

### Effects of CIH on cardiac function

CIH produced an increase ($\sim$13 mm Hg) in RVSP at day 21 days, which remained elevated at 28 days of exposure. Indeed, after 21 days of CIH, RVSP was significatively higher related to the controls ($32.7 \pm 2.3$ vs. $19.7 \pm 3.2$ mmHg, respectively,

$p < 0.05$; Fig. 1a). Meanwhile, the HR remained unchanged during CIH exposure (Fig. 1b).

Fig. 2 shows the effects of CIH for 28 days on cardiac function measured by MRI. Fig. 2a shows representative images of axial and longitudinal views (left panel) and representative images of end-diastolic and systolic phases in a rat exposed to CIH for 28 days and a control age-matched rat. Rats exposed to CIH for 28 showed a higher right ventricular wall thickness (RVWT) and a right ventricle end-systolic volume (RVESV) related to the control animals, without changes on the right ventricle end-diastolic volume (RVEDV) and EF (Fig. 2b). CIH did not modify these parameters in the left ventricle (Fig. 2c).

### Vasoactive contractile response to KCl and endothelin-1 of isolated pulmonary arteries from rats exposed to CIH

CIH produced a progressive increase in the maximal contraction evoked by KCl and ET-1 in pulmonary arteries of 2nd–3rd order. Isolated small pulmonary ($\sim$300–400 µm) arteries harvested from rats exposed to 21 and 28 days to CIH showed a higher maximal contraction in response to increasing KCl
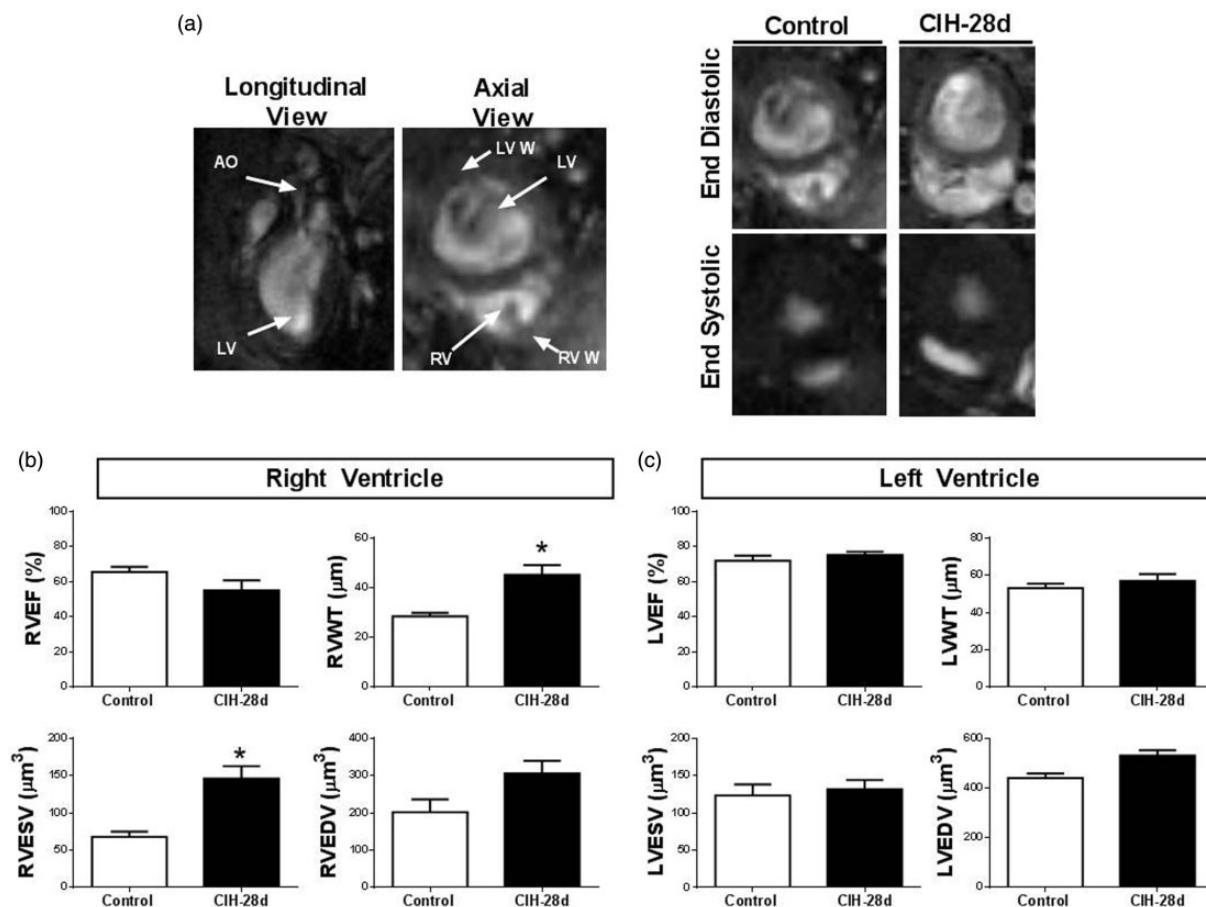
**Fig. 2.** Effects of CIH on cardiac function. Animals were exposed to 28d-CIH, and the MRI study was assessed. (a) Left panel: representative images of axial and longitudinal view. Right panel: representative images of axial view, in the end-diastolic and systolic phase. (b) Right ventricular data of ejection fraction (RVEF, %), free wall thickness (RVWT, μm), end-systolic (RVESV) and end-diastolic volume (RVEDV, μm$^3$). (c) Left ventricular ejection fraction (LVEF, %), free wall thickness (LVWT, μm), end-systolic (LVESV), and end-diastolic volume (RVEDV, μm$^3$) in control animals (empty bar, $n = 3$) or exposed to 28 days to CIH (black bar, $n = 3$). Ejection fraction: (end diastolic volume − end systolic volume)/end-diastolic volume × 100; free wall thickness: (pericardium area − endocardium area) × ventricular length; end systolic and diastolic volume: (end systolic or diastolic area × ventricular length). AO: aorta; LV: left ventricle; RV: right ventricle; LVW: left ventricular wall; RVW: right ventricular wall. Right ventricular free wall thickness (RVWT), left ventricular free wall thickness (LVWT), right ventricle end-systolic volume (RVESV), left ventricle end-systolic volume (LVESV), right ventricle end-diastolic volume (RVEDV), left ventricle end-diastolic volume (RVEDV). Control (empty bar), 28 days CIH (black bars). Values are mean ± SE. *$p < 0.05$ vs. control. Student's unpaired $t$ test.

concentration, with a lower EC50 as compared to arteries from control animals (Fig. 3a). The maximal response to ET-1 of isolated pulmonary arteries from rats exposed to CIH for 21 and 28 days increased by ∼4 and ∼6 times, respectively, as related to the control group, while the half maximal effective concentration (pEC$_{50}$) remained unchanged (Fig. 3b). Interestingly, when the maximal contractile response to ET-1 was expressed as a percentage of the maximal response to KCl, the differences between control and CIH-treated arteries disappeared, presenting similar values of maximal normalized contraction and pEC$_{50}$ (Fig. 3c).

## Pulmonary vascular remodeling induced by CIH

Fig. 4 summarized the increase of the percentage of the medial layer thickness of small pulmonary arteries (150–300 μm) induced by CIH. The increase of the thickness of the medial layer was significant at 21 days of CIH exposure (66.2 ± 2.4%) and remained augmented at 28 days of CIH (64.7 ± 4.0%) as compared to arteries from CIH-rats treated for 14 days (50.8 ± 1.5%) and from control rats (45.0 ± 1.6%).

## Effects of CIH on the expression of pulmonary gene expression of STOC-forming subunits

Lungs from rats exposed to CIH for 14, 21, and 28 days showed a higher relative lung gene expression of TRPC1 and TRPC6 compared to the control group (Fig. 5a and c). On the contrary, we found a higher expression of TRPC4 and ORAI1 subunits only in the lungs from rats exposed to 28 days as compared to controls (Fig. 5b
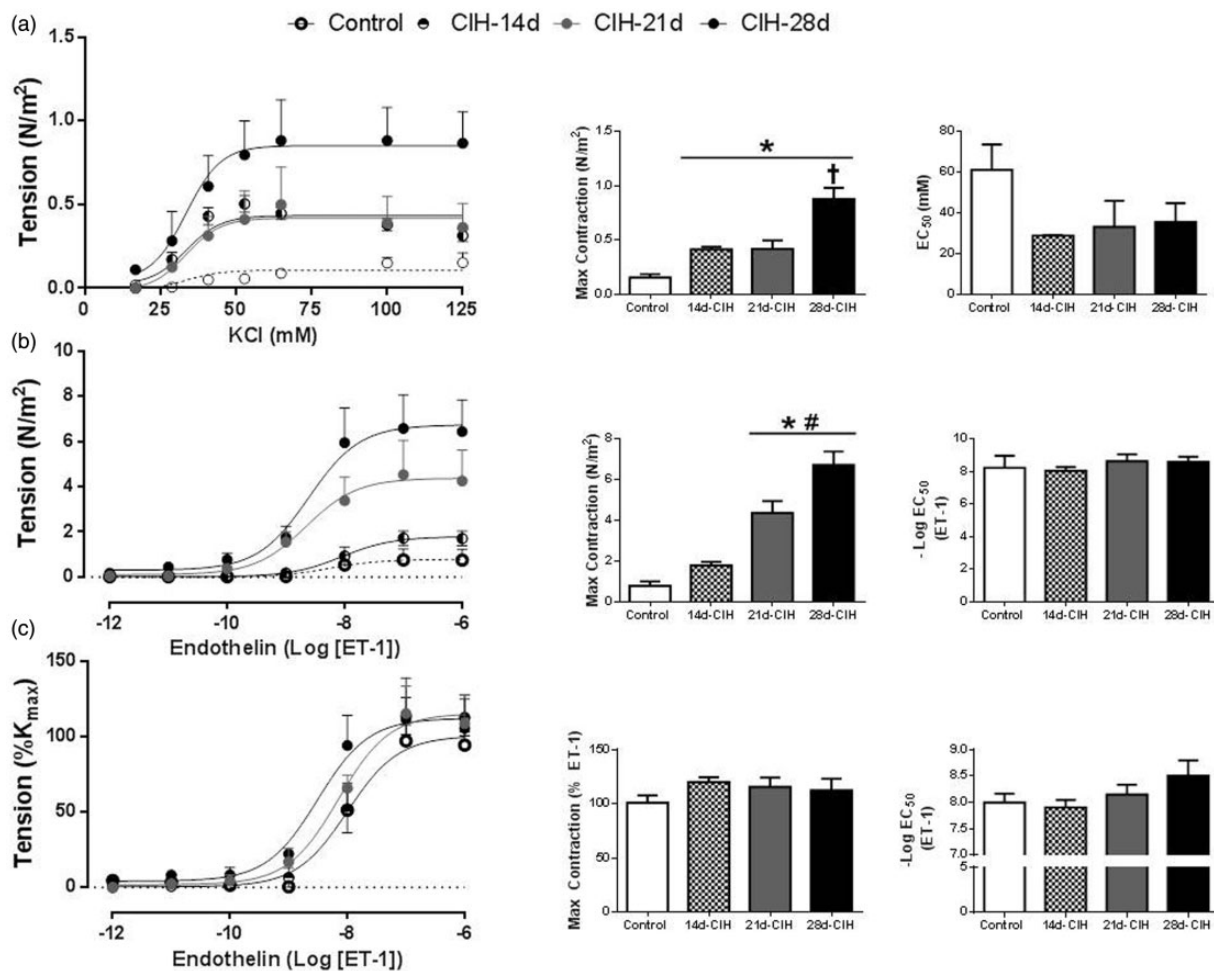
**Fig. 3.** Vasoconstrictor effect of KCl and ET-1 in isolated pulmonary arteries. Small pulmonary arteries (2nd branch generation) isolated 24 h from rats exposed to 14, 21 or 28 days of CIH and control rats were induced to contract by increasing concentrations of KCl (a), endothelin-1 (b) and endothelin-1 normalized by the contractile effect induced by KCl 40 mM (% Kmax) (c). 14d-CIH (half circles, $n = 3$), 21d-CIH (gray circles, $n = 5$) and 28d-CIH (black circles, $n = 5$). The corresponding maximal contraction and potency were calculated for KCl, ET-1 and ET-1 (%KCl). Values are mean ± SE. *$p < 0.05$ vs. control, #$p < 0.05$ vs. 14d-CIH, one-way ANOVA and Newman–Keuls post-test.

and d). The relative expression of ORAI 2 was not affected by CIH (Fig. 5e).

## Effect of CIH on the lung protein levels of the STOC-forming subunits

Lungs from rats exposed to CIH for 28 days showed higher levels of TRPC6, STIM1, and ORAI1 proteins compared to controls (Fig. 6b–e). The protein levels of TRPC1 and ORAI2 remained unchanged during CIH exposure (Fig. 6a and d).

## Discussion

Our results showed that exposure of rats to CIH for 14–28 days progressively enhanced the vasoconstrictor response to KCl and ET-1 in small pulmonary arteries ex vivo, produced vascular pulmonary remodeling, increased RVSP, increased RVWT and RVESV, measured by MRI.

Accordingly, present results agree and extend previous observation that exposure of rats to CIH ($O_2$ 4–8%, 8 h/day) for 28 days increased RVSP ($\sim$35.0 to 37.5 mmHg), augmented the Fulton's index and produces pulmonary arterial remodeling.[12,13] An important contribution of our results is the observation that shorter times of CIH, than previously tested result in pathological cardiopulmonary changes. RVSP and medial layer area increased at day 21 of CIH, while contractile hyperreactivity to potassium and ET1 increased at 14 days and 21 days of CIH, respectively. The contraction in response to KCl is related to either the amount muscle layer of the vessels or to the function of voltage-dependent contraction mechanisms like L- or T-type channels.[30,40] On the other hand, the contraction in response to ET-1 is primarily related to mobilization of sarcoplasmic reticulum $Ca^{2+}$ stores, but it can be subsequently associated to STOC activation resulting from store depletion.[18,24] Collectively, these data suggest that increased KCl-induced contraction at 14 days may be the result of
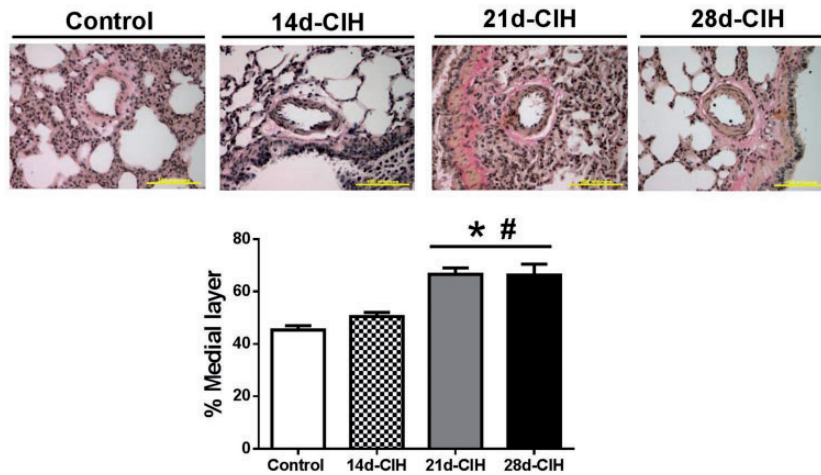
**Fig. 4.** Pulmonary vascular remodeling on small pulmonary arteries in response to CIH. Representative images of small pulmonary arteries of ~150–200 μM of diameter stained with Van Gieson. Quantification of the % medial layer of small pulmonary arteries in control (empty bar, $n = 6$), 14d-CIH (lined bar, $n = 6$), 21d-CIH (gray bar, $n = 7$) and 28d-CIH (black bar, $n = 7$). The medial layer was calculated as (Muscular area-lumen area)/Muscular area × 100. Bar = 100 μm. Values are mean ± SE. *$p < 0.05$ vs. control, #$p < 0.05$ vs. 14d-CIH. One-way ANOVA and Newman–Keuls post-test.
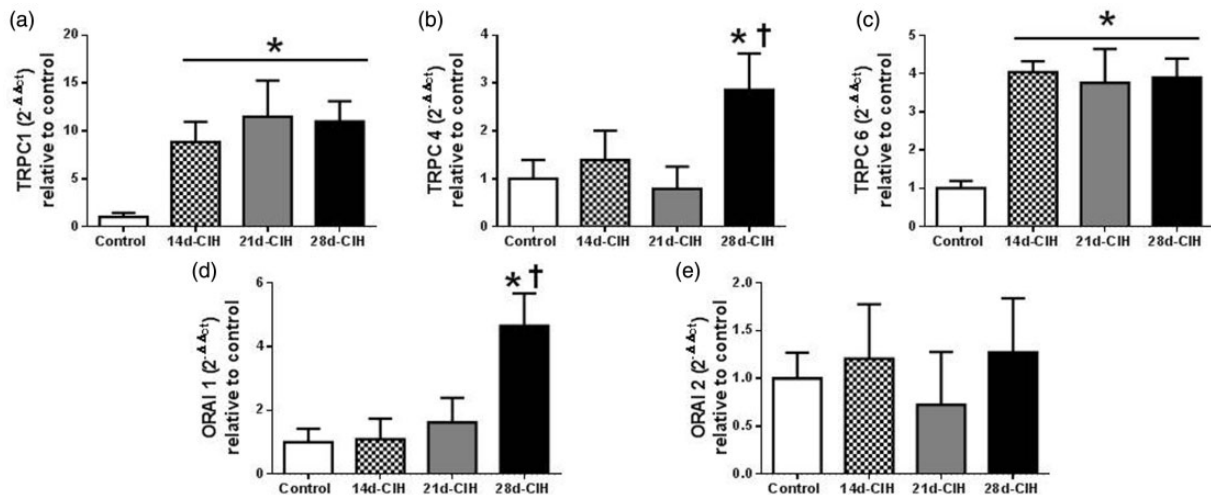


**Fig. 5.** Effect of CIH on pulmonary relative gene expression of STOC-forming subunits in rats. Pulmonary gene expression of (a) TRPC1, (b) TRPC4, (c) TRPC6, (d) ORAI1, and (e) ORAI 2 of control (empty bar, $n = 6$), 14d-CIH (lined bar, $n = 6$), 21d-CIH (gray bar, $n = 7$), and 28d-CIH (black bar, $n = 7$) animals. Values are expressed as $2-\Delta\Delta CT$ in relation to the control. Values are mean ± SE. *$p < 0.05$ vs. control, †$p < 0.05$ vs. all. One-way ANOVA and Newman–Keuls post-test.

up-regulated L- or T-type channels, while the increase in arterial smooth muscle contributes to enhance potassium contractility from day 21. On the other hand, ET-1 hyperreactivity matches with the appearance of pulmonary arterial wall thickening and RVSP increase at day 21, suggesting that later, ET-1 signaling, and probably STOC associated Ca2+ entry is necessary for pulmonary arterial hypertension and pathological remodeling in response to CIH. Previous studies in systemic arteries from CIH rats show that impaired vascular function occurs by, either, decreased endothelial-dependent relaxation and, increased constrictor response to KCl, which also correlates with arterial wall

thickness.[32,33] However, it is worth to note that this study did not address the contribution of relaxing agents derived from the endothelium, and its contribution to the pulmonary vascular dysfunction cannot be ruled out. In addition, we have found that CIH increased the pulmonary gene expression of the TRPC1 and TRPC6 channels at 14 days of CIH, while the expression of TRPC4 and ORAI1 subunits increased in rats exposed to CIH for 28 days. Similarly, the lung tissue from CIH-rats for 28 days expressed higher protein levels of TRPC6, STIM1, and ORAI1, while the levels of TRPC1 and ORAI2 remained unchanged during CIH exposure. Thus, the changes in
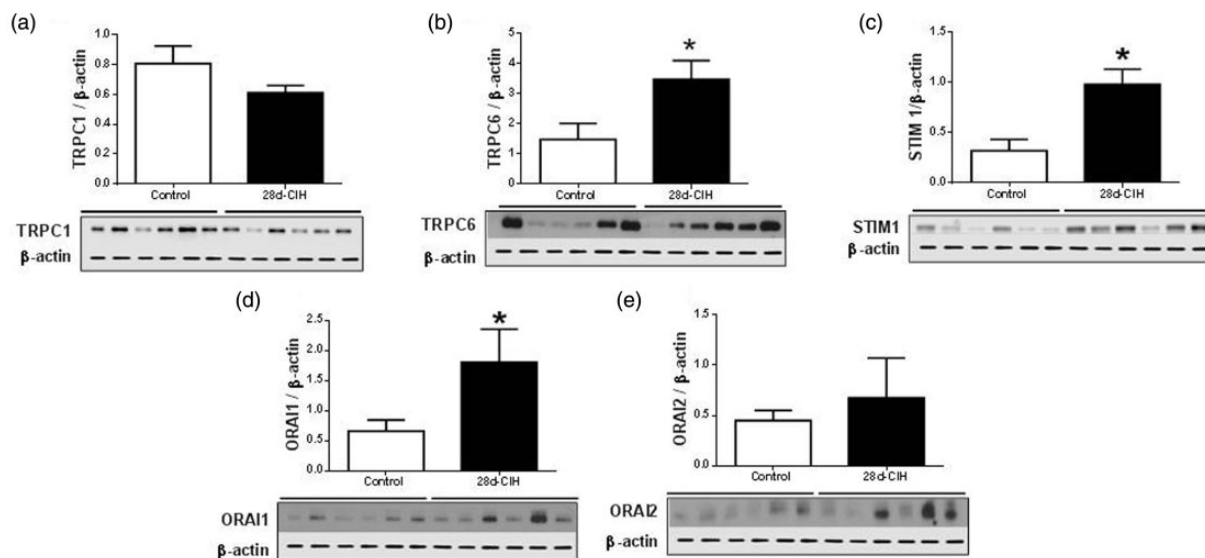
**Fig. 6.** Effect of the exposure to 28 days to CIH of the protein levels on STOC-forming subunits in the lungs. Quantification of the protein levels of (a) TRPC1, (b) TRPC6, (c) STIM1, (d) ORAI2, and (e) ORAI1 on control (empty bar, $n = 6$) and CIH-28d (black bar, $n = 6$) animals. Values are expressed as a ratio of β-actin. Values are mean ± SE. *$p < 0.05$ vs. control. Student's unpaired $t$ test.

expression of STOC subunits paralleled the morphological and functional vascular pulmonary changes induced by CIH. The profile of STOC subunits induced by hypoxia depends on the time of exposure, the experimental preparation and the development: up-regulation of Orai1 and 2 is reported in de-endothelized pulmonary arteries from rats submitted to 21 days of sustained hypoxia,[29] overexpression of Stim1, TRPC1, and Orai1 is observed in cultured PASMC submitted to 12–48 h of hypoxia,[41] induction of Stim1, Stim2, Orai1, Orai2, and TRPC6 expression takes place in PASMC submitted to 72 h of hypoxia,[26] while TRPC4 and Stim1 increase is described in lungs from newborn sheep submitted to hypobaric hypoxia during gestation and early growth.[24] The increase in pulmonary gene and protein STOC subunits expression induced by CIH reported here, partially agrees with these observations. However, further studies are required to determine if the same changes occur specifically in PASMC pulmonary artery endothelial or fibroblast cells, or in other non-vascular tissues in our model.

It is well known that sustained hypoxia produces pulmonary vascular remodeling featured by hypertrophy and/or hyperplasia of PASMC, leading to vasoconstriction and PH.[17] Similarly, CIH produced pulmonary vascular remodeling and hypertension. It has been proposed that oxidative stress and activation of inflammatory pathways are involved in the pulmonary vascular alterations induced by CIH.[12–14] We have previously demonstrated that the CIH pattern used in this study produces systemic oxidative stress[31] and endothelial dysfunction.[32,33] High levels of ROS raise $[Ca^{2+}i]$, in PASMC, which is the key factor in differentiation and proliferation of vascular smooth muscle.[42,43] In PASMC, [Ca2+i] may increase by the activation of two mechanisms: (1) release of Ca2+ from the sarcoplasmic reticulum, mediated by intracellular channels sensitive to

inositol trisphosphate (IP3) or by ryanodine receptors (RyR), or (2) by the entry of Ca2+ from the extracellular space mediated by the Na+/Ca2 exchanger, Ca2+ type L channels, and stretch-activated Ca2+ channels. In addition, Stim-activated TRPC-ORAI channels play a key role in homeostasis of the intracellular $[Ca^{2+}i]$, which is crucial for the contraction and pathological pulmonary arterial remodeling, including the migration, differentiation, and proliferation of myocytes and pulmonary arterial fibroblasts in response to acute and sustained hypoxia.[18,19,23–25,28,29,44] The available evidence suggests that the increased $[Ca^{2+}i]$ and vasoconstriction in response to acute hypoxia and ET-1 depended on STOC.[19,23,24,28]

In conclusion, present results show that pulmonary vascular dysfunction resulting from CIH occurs via a progressive increase in contractile reactivity and remodeling of pulmonary arteries, affecting at long term the right ventricular function. Furthermore, these changes are paralleled by increased expression of lung TRPCs and ORA1, suggesting a crucial role for STOC in the development of pulmonary vascular remodeling and pulmonary hypertension induced by CIH. Further studies are needed to determine the role of STOC in CIH-induced PH.

## Conflict of interest

The author(s) declare that there is no conflict of interest.

## Funding

## ORCID iD

R. Iturriaga  https://orcid.org/0000-0001-5387-9897

## References

1. Young T, Finn L, Peppard PE, et al. Sleep disordered breathing and mortality: eighteen-year follow-up of the Wisconsin sleep cohort. *Sleep* 2008; 31: 1071–1078.
2. Somers VK, White DP, Amin R, et al. Sleep apnea and cardiovascular disease. *Circulation* 2008; 118: 1080–1111.
3. Ferini-Strambi L, Baietto C, Di Gioia MR, et al. Cognitive dysfunction in patients with obstructive sleep apnea (OSA): partial reversibility after continuous positive airway pressure (CPAP). *Brain Res Bull* 2003; 61: 87–92.
4. Dempsey JA, Veasey SC, Morgan BJ, et al. Pathophysiology of sleep apnea. *Physiol Rev* 2010; 90: 47–112.
5. Garvey JF, Taylor CT and McNicholas WT. Cardiovascular disease in obstructive sleep apnoea syndrome: the role of intermittent hypoxia and inflammation. *Eur Respir J* 2009; 33: 1195–1205.
6. Bosc LVG, Resta T, Walker B, et al. Mechanisms of intermittent hypoxia induced hypertension. *J Cell Mol Med* 2010; 14: 3–17.
7. Me AS, El-Desoky ME, Maaty AER, et al. Pulmonary hypertension in obstructive sleep apnea hypopnea syndrome. *Egypt J Chest Dis Tuber* 2013; 62: 459–465.
8. Floras JS. Sleep apnea and cardiovascular disease: an enigmatic risk factor. *Circ Res* 2018; 122: 1741–1764.
9. Imran TF, Ghazipura M, Liu S, et al. Effect of continuous positive airway pressure treatment on pulmonary artery pressure in patients with isolated obstructive sleep apnea: a meta-analysis. *Heart Fail Rev* 2016; 21: 591–598.
10. Iturriaga R, Del Rio R, Idiaquez J, et al. Carotid body chemoreceptors, sympathetic neural activation, and cardiometabolic disease. *Biol Res Biol Res* 2016; 49: 13.
11. Iturriaga R, Oyarce MP and Dias ACR. Role of carotid body in intermittent hypoxia-related hypertension. *Curr Hyperten Rep* 2017; 19: 38.
12. Jin H, Wang Y, Zhou L, et al. Melatonin attenuates hypoxic pulmonary hypertension by inhibiting the inflammation and the proliferation of pulmonary arterial smooth muscle cells. *J Pineal Res* 2014; 57: 442–450.
13. Nara A, Nagai H, Shintani-Ishida K, et al. Pulmonary arterial hypertension in rats due to age-related arginase activation in intermittent hypoxia. *Am J Respir Cell Mol Biol* 2015; 53: 184–192.
14. Nisbet RE, Graves AS, Kleinhenz DJ, et al. The role of NADPH oxidase in chronic intermittent hypoxia-induced pulmonary hypertension in mice. *Am J Respir Cell Mol Biol* 2009; 40: 601–609.
15. Iturriaga R and Castillo-Galán S. Potential contribution of carotid body-induced sympathetic and renin-angiotensin system overflow to pulmonary hypertension in intermittent hypoxia. *Curr Hyperten Rep* 2019; 21: 89.
16. Suresh K and Shimoda LA. Lung circulation. *Compr Physiol* 2016; 6: 897–943.
17. Sylvester JT, Shimoda LA, Aaronson PI, et al. Hypoxic pulmonary vasoconstriction. *Physiol Rev* 2012; 92: 367–520.
18. Reyes RV, Castillo-Galán S, Hernandez I, et al. Revisiting the role of TRP, Orai, and ASIC channels in the pulmonary arterial response to hypoxia. *Front Physiol* 2018; 9: 486.
19. Weigand L, Foxson J, Wang J, et al. Inhibition of hypoxic pulmonary vasoconstriction by antagonists of store-operated Ca2+ and nonselective cation channels. *Am J Physiol Lung Cell Mol Physiol* 2005; 28: L5–L13.
20. Fuchs B, Dietrich A, Gudermann N, et al. The role of classical transient receptor potential channels in the regulation of hypoxic pulmonary vasoconstriction. *Membr Recept Channels Transporters Pulm Circ* 2010; 661: 187–200.
21. Jernigan NL, Paffett ML, Walker BR, et al. ASIC1 contributes to pulmonary vascular smooth muscle store-operated Ca2+ entry. *Am J Physiol Lung Cell Mol Physiol* 2009; 297: 271–285.
22. Wray S and Burdyga T. Sarcoplasmic reticulum function in smooth muscle. *Physiol Rev* 2010; 90: 113–178.
23. Castillo-Galán S, Quezada S, Moraga FA, et al. 2-Aminoethyl-diphenylborinate modifies the pulmonary circulation in pulmonary hypertensive newborn lambs partially gestated at high altitude. *Am J Physiol Lung Cell Mol Physiol* 2016; 311: L788–L799.
24. Parrau D, Ebensperger G, Herrera EA, et al. Store-operated channels in the pulmonary circulation of high-and low-altitude neonatal lambs. *Am J Physiol Lung Cell Mol Physiol* 2013; 304: L540–L548.
25. Golovina VA, Platoshyn O, Bailey CL, et al. Upregulated TRP and enhanced capacitative Ca2+ entry in human pulmonary artery myocytes during proliferation. *Am J Physiol Heart Circ Physiol* 2001; 280: H746–H755.
26. He X, Song S, Ayon RJ, et al. Hypoxia selectively upregulates cation channels and increases cytosolic [Ca2+] in pulmonary, but not coronary, arterial smooth muscle cells. *Am J Physiol Cell Physiol* 2018; 314: C504–C517.
27. Hou X, Chen J, Luo Y, et al. Silencing of STIM1 attenuates hypoxia-induced PASMCs proliferation via inhibition of the SOC/Ca2+/NFAT pathway. *Respir Res* 2013; 14: 2.
28. Lu W, Wang J, Shimoda LA, et al. Differences in STIM1 and TRPC expression in proximal and distal pulmonary arterial smooth muscle are associated with differences in Ca2+ responses to hypoxia. *Am J Physiol Lung Cell Mol Physiol* 2008; 295: L104–L113.
29. Wang J, Xu C, Zheng K, et al. Orai 1,2,3 and STIM1 promote store-operated calcium entry in pulmonary arterial smooth muscle cells. *Cell Death Discov* 2017; 3: 17074.
30. Reyes RV, Díaz M, Ebensperger G, et al. The role of nitric oxide in the cardiopulmonary response to hypoxia in highland and lowland newborn llamas. *J Physiol* 2018; 596: 5907–5923.
31. Del Rio R, Moya EA and Iturriaga R. Carotid body and cardiorespiratory alterations in intermittent hypoxia: the oxidative link. *Eur Respir J* 2010; 36: 143–150.
32. Krause BJ, Del Rio R, Moya EA, et al. Arginase/eNOS imbalance contributes to endothelial dysfunction in chronic intermittent hypoxia in rats. *J Hypertension* 2015; 33: 515–524.
33. Krause BJ, Casanello P, Dias ACR, et al. Chronic intermittent hypoxia-induced vascular dysfunction in rats is reverted by N-acetylcysteine supplementation and arginase inhibition. *Front Physiol* 2018; 9: 901.
34. Lavin B, Lacerda S, Andia ME, et al. Tropoelastin: an in vivo imaging marker of dysfunctional matrix turnover during abdominal aortic dilation. *Cardiovasc Res* 2020; 116: 995–1005.
35. Mulvany MJ and Aalkjaer C. Structure and function of small arteries. *Physiol Rev* 1990; 70: 921–961.

36. Delaey C, Boussery K and Van de Voorde J. Contractility studies on isolated bovine choroidal small arteries: determination of the active and passive wall tension-internal circumference relation. *Exp Eye Res* 2002; 75: 243–248.

37. Cañas D, Herrera EA, García-Herrera C, et al. Fetal growth restriction induces heterogeneous effects on vascular biomechanical and functional properties in guinea pigs (*Cavia porcellus*). *Front Physiol* 2017; 8: 144.

38. Herrera EA, Riquelme RA, Ebensperger G, et al. Long-term exposure to high-altitude chronic hypoxia during gestation induces neonatal pulmonary hypertension at sea level. *Am J Physiol Regul Integr Comp Physiol* 2010; 299: R1676–R1684.

39. Glantz SA and Slinker K. *Primer of applied regression and analysis of variance*. New York, NY: McGraw-Hill, 2001, pp.418–507.

40. Wan J, Yamamura A, Zimnicka AM, et al. Chronic hypoxia selectively enhances L- and T-type voltage-dependent Ca2+ channel activity in pulmonary artery by upregulating Ca1.2 and Ca3.2. *Am J Physiol Lung Cell Mol Physiol* 2013; 305: L154–L164.

41. Chen TX, Xu XY, Zhao Z, et al. Hydrogen peroxide is a critical regulator of the hypoxia-induced alterations of store-operated Ca2+ entry into rat pulmonary arterial smooth muscle cells. *Am J Physiol Lung Cell Mol Physiol* 2017; 312: L477–L487.

42. Shao J, Wang P, Liu A, et al. Punicalagin prevents hypoxic pulmonary hypertension via anti-oxidant effects in rats. *Am J Chin Med* 2016; 44: 785–801.

43. Waypa GB, Marks JD, Mac MM, et al. Mitochondrial reactive oxygen species trigger calcium increases during hypoxia in pulmonary arterial myocytes. *Circulation Res* 2002; 91: 719–726.

44. Guibert C, Ducret T and Savinea, JP. Expression and physiological roles of TRP channels in smooth muscle cells. In: *Transient receptor potential channels*. Dordrecht: Springer, 2011, pp.687–706.